The Astrophysical Journal, 682:690–696, 2008 July 20

EVIDENCE FOR MASS-PER-CHARGE–DEPENDENT ACCELERATION OF A MULTIPLE-COMPONENT SEED POPULATION BY CME-DRIVEN INTERPLANETARY SHOCKS NEAR 1 AU

F. Allegrini and M. I. Desai
Southwest Research Institute, San Antonio, TX 78238

G. M. Mason
Applied Physics Laboratory, The Johns Hopkins University, Laurel, MD 20723

and

H. Kucharek and E. Möbius
Space Science Center, University of New Hampshire, Durham, NH 03824
Received 2007 October 25; accepted 2008 January 31

ABSTRACT

Using measurements from the ULEIS and SEPICA instruments on board the *Advanced Composition Explorer* between 1997 November and 2000 October, we have surveyed the abundances of 0.25–0.8 MeV nucleon^{-1} He^+, ^{3}He, and heavy ions from C-Fe during 18 CME-driven interplanetary (IP) shocks observed near 1 AU. Our results show that each of the 18 IP shocks is accompanied by enhancements in the intensities of both ^{3}He and He^+ ions. In addition we find that, on a case-by-case basis, the abundances of He^+ and the heavier elements such as C-Fe (but not ^{3}He) are depleted systematically as a function of the ion's M/Q ratio when compared with those measured in the ambient suprathermal ion population upstream of the IP shocks. These results show for the first time that individual IP shocks routinely accelerate ions from multiple seed populations, such as multiple solar energetic particle events, corotating interaction regions, pickup ions, etc., via systematic rigidity-dependent acceleration processes where ions with higher rigidity or M/Q ratios are accelerated less efficiently than those with lower M/Q ratios. We also compare the M/Q-dependent depletion of these abundances with the locally measured shock parameters and explore why the ^{3}He abundance does not fit into the systematic M/Q-charge-dependent fractionation processes.

Subject headings: acceleration of particles — interplanetary medium — Sun: coronal mass ejections (CMEs)

1. INTRODUCTION

In situ measurements of energetic particles, plasmas, and magnetic fields in the vicinity of coronal mass ejection (CME)–driven interplanetary (IP) shocks near 1 AU have been routinely used to test predictions of shock acceleration theories in detail over the last five decades (e.g., Kennel et al. 1986; van Nes et al. 1984; Desai et al. 2003; Lario et al. 2005). Prior to the 1990s the ion intensity enhancements associated with such IP shocks were believed to occur due to the diffusive acceleration of ambient solar wind ions by the shocks as they moved through the IP medium (e.g., Lee 1983; Forman & Webb 1985). However, using isotopic composition data from the *Advanced Composition Explorer* (*ACE*) Ultra Low Energy Isotope Spectrometer (ULEIS), Desai et al. (2001, 2003) found large enrichments of ^{3}He ions over the solar wind value in more than half of the IP shock events they surveyed. Over the same period, Kucharek et al. (2003) surveyed the ionic composition of He from the *ACE* Solar Energetic Particle Ionic Charge Analyzer (SEPICA) and found strongly enhanced abundances of He^+ ions during many CME-driven IP shock events. Since both ^{3}He and He^+ ions are extremely rare in the solar wind (relative abundance ratios are $\sim 4 \times 10^{-4}$; see Gloeckler & Geiss 1998a), these results provide compelling evidence that the seed population for IP shocks contains suprathermal material from a variety of sources that include flare-accelerated ^{3}He-rich material and interstellar pickup He^+ ions.

Desai et al. (2003) also surveyed the elemental composition of C-Fe ions and found that the average C-Fe abundances in IP shock events were systematically depleted according to the ion's mass-per-charge ratio when compared with the corresponding average values measured in the suprathemal ion population upstream of the shocks. Desai et al. (2003) interpreted these depletions as being consistent with rigidity-dependent shock acceleration mechanisms (Lee 2005) where ions with higher M/Q values are accelerated less efficiently than those with lower M/Q values (also see Klecker et al. 1981, 2000, 2003; Tylka et al. 1999).

However, the Desai et al. (2001, 2003) and Kucharek et al. (2003) studies were carried out independently. Consequently, at present it is not clear whether the same IP shock can accelerate ^{3}He and He^+ ions from distinct sources via the same rigidity-dependent shock acceleration processes. In this paper we survey the $\sim$0.25–0.8 MeV nucleon^{-1} ^{3}He, He^+, and C-Fe abundances measured by ULEIS and SEPICA during several IP shock events observed at *ACE* from 1997 November to 2000 October. Specifically, we investigate whether a single IP shock can accelerate ions from multiple sources via the same rigidity-dependent acceleration processes. Finally, we discuss our results in terms of the variability of the seed population and the physical nature of the shock acceleration processes.

2. INSTRUMENTATION

We use suprathermal through energetic particle measurements between 0.25 and 0.80 MeV nucleon^{-1} obtained by high-resolution mass spectrometers ULEIS and SEPICA on board *ACE* (Stone et al. 1998). ULEIS and SEPICA can resolve the helium isotopes ^{3}He and ^{4}He and ionic charge states He^+ and He^{2+}, respectively, even when the corresponding ratios fall below the 1% level. Both instruments measure He ions in comparable energy ranges between $\sim$0.25 and 2.0 MeV nucleon^{-1}. In addition, ULEIS can measure the elemental abundances of C to Ni. For a more detailed

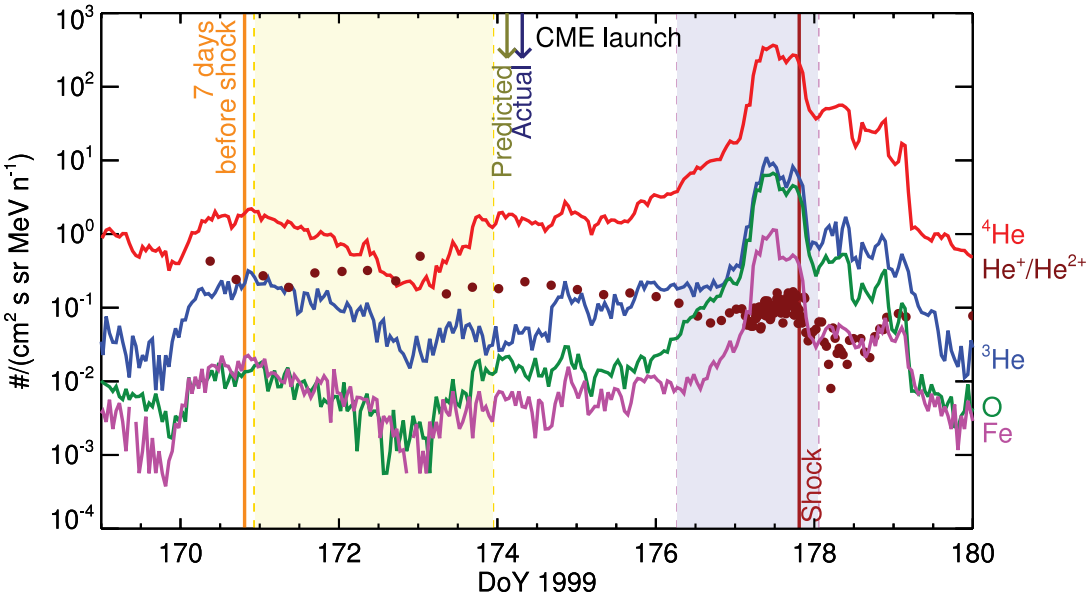

FIG. 1.—Hourly averaged intensity profiles of 0.25–0.80 MeV nucleon^{-1} ^{3}He, ^{4}He, O, and Fe (*solid lines*) measured by *ACE* ULEIS and the He^+/He^{2+} ratio (*filled circles*) measured by SEPICA for event 5 of Table 1. The yellow-shaded region shows the ambient interval, the purple-shaded region shows the shock interval, the brown line represents the shock arrival at *ACE*, and the arrows show the estimated and actual CME launch.

description of these instruments, see Mason et al. (1998) and Möbius et al. (1998).

3. OBSERVATIONS

In this study we select 18 CME-driven IP shocks during the period from 1997 November to 2000 October. These events are a subset of those surveyed by Desai et al. (2003), who selected their events on the basis of the following criteria: (1) the 0.5–2.0 MeV nucleon^{-1} ^{4}He, O, and Fe intensities increase by a factor of 5; (2) the intensity-time profiles track each other; and (3) no velocity dispersion during onsets. In order to focus on events with multiple seed populations, for this work we selected events from the list of Desai et al. (2003) that also had SEPICA data coverage and measurable levels of He^+ and ^{3}He.

Figure 1 shows intensity-time profiles for ^{3}He, ^{4}He, He^+/He^{2+}, O, and Fe in the 0.25–0.80 MeV nucleon^{-1} energy range measured by *ACE* ULEIS and SEPICA for the day of year 177, 1999 IP shock (*brown line*). The purple band represents the shock-associated sampling interval. The yellow band represents the sampling interval used to give us a proxy of the ambient suprathermal ion abundances. We selected upstream intervals corresponding to all 18 events on the basis of the following: (1) the interval should start within 7 days of the shock arrival, and (2) it should end before (or at) the estimated or actual launch time of the CME that we determined was most likely responsible for driving the IP shock.

We first estimated the CME launch time by using the measured shock speed at 1 AU and propagating it back to the Sun. We then identified the CME[1] that most likely generated the shock and obtained its actual launch time from the Sun. In most cases (12 out of 18), the estimated launch time occurred before the actual CME launch time, probably because the IP shocks decelerated en route to L1. These criteria have enabled us to select the upstream intervals that fall within ~1 week of the IP shock event. Furthermore, these upstream intervals are also unlikely to contain particles that were accelerated by the same IP shock when it was near the Sun. We believe that the ion composition measured in these upstream intervals provides us with a reasonable proxy for the suprathermal ion population that the associated IP shock could have encountered en route to Earth (also see Desai et al. 2003).

Figure 2 shows the 0.25–0.8 MeV nucleon^{-1} (1) He mass histogram and (2) He ionic charge state distribution, measured by ULEIS and SEPICA, respectively, during the shock sampling interval in Figure 1 (*purple band*). Note that both the ^{3}He and He^+ peaks are well separated from the more abundant ^{4}He; the $^3He/^4He$ ratio is 0.00439 ± 0.00028, and the He^+/He^{2+} ratio is 0.0853 ± 0.0005. In other words, the ratios are enhanced by more than a factor of ~10 and ~1700, respectively, over the corresponding values measured in the solar wind ($^3He/^4He \sim 0.000408 \pm 0.000025$, Gloeckler & Geiss 1998a; $He^+/He^{2+} < 0.00005$, Gloeckler & Geiss 1998b).

Table 1 lists the 18 selected events with the shock arrival time at 1 AU (seen at *ACE* where available, or at *WIND* otherwise) in column (2); the sampling time interval for the shock interval in column (3); the corresponding $^3He/^4He$, He^+/He^{2+}, and Fe/O ratios in columns (4)–(6); the sampling time interval for the upstream interval in column (7); the corresponding $^3He/^4He$, He^+/He^{2+}, and Fe/O ratios in columns (8)–(10); the proton density compression ratio in column (11); the shock speed in the upstream frame in column (12); and the shock normal angle in column (13).[2] The $^3He/^4He$ and He^+/He^{2+} ratios are between 0.25 and 0.80 MeV nucleon^{-1}, and the Fe/O ratios are between 0.35 and 0.80 MeV nucleon^{-1}.

Figure 3 investigates the relationship between the shock-accelerated abundances and the corresponding upstream abundances as a function of the ion's M/Q ratio for two IP shock events, namely, (1) event 5 on 1999 June 26, 1931 UT, and (2) event 6 on 1999 July 6, 1425 UT. The mean ionization states for the heavy

[1] From the *SOHO* LASCO CME Catalog at http://cdaw.gsfc.nasa.gov/CME_list/index.html.

[2] The shock parameters are taken from the *ACE* Lists of Disturbances and Transients, maintained by C. W. Smith (http://www-ssg.sr.unh.edu/mag/ace/ACElists/obs_list.html), when available, or otherwise from the Interplanetary Shock Database from the MIT Space Plasma Group (http://space.mit.edu/home/jck/shockdb/shockdb.html).

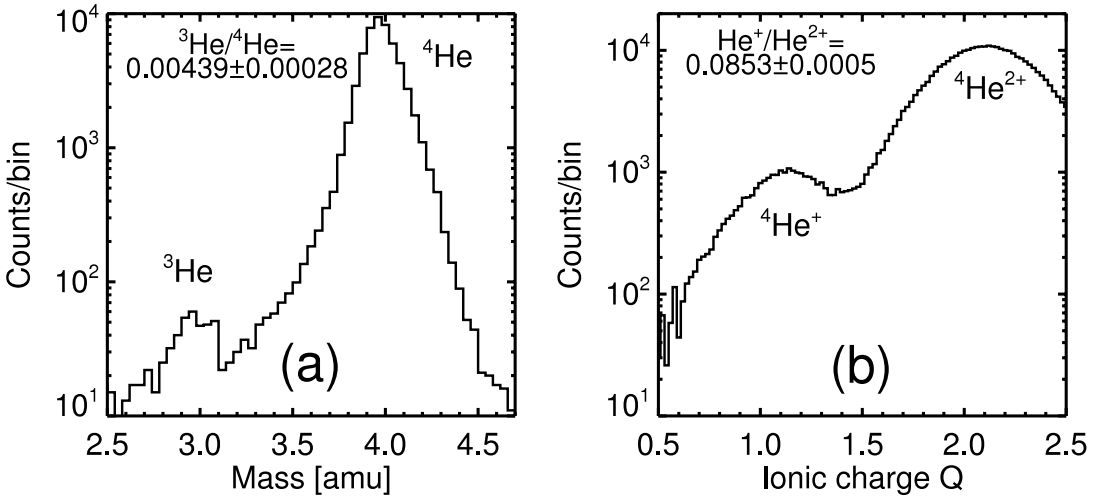

FIG. 2.—(*a*) Mass histogram from ULEIS and (*b*) charge state histogram from SEPICA showing the well-resolved ^{3}He and He$^+$ peaks for the event of Fig. 1 (event 5 of Table 1).

ions are taken as the average values measured in gradual solar energetic particles (SEPs; Klecker et al. 1999; Möbius et al. 1999, 2000). We have chosen average charge states here for this first limited study because the main trend of the charge states with species remains the same even if all charge states in an SEP event shift to higher or lower values (Möbius et al. 2000). The solid lines indicate linear fits to the log of the data points (^{3}He not included). The figure clearly shows that the shock-accelerated heavy abundances from C-Fe, ^{4}He, and He$^+$ ions are systematically depleted according to the M/Q ratio when compared with the corresponding values measured upstream of the shocks. Note, however, that the ^{3}He abundances in both events do not follow the trend and are in fact depleted when compared with the corresponding upstream values.

By performing a similar analysis for all 18 IP shock events in our survey, we found the following: (1) In 15 out of 18 events the trend is similar to that shown in Figure 3; i.e., the IP shock abundances are systematically depleted with respect to M/Q. (2) In 12 out of 18 events ^{3}He falls under the line; in 3 events the ^{3}He data point falls on the line, and in 3 events it lies above the line. (3) In 7 out of 12 events He$^+$ falls on the line; in 2 events the He$^+$ data point falls below the line, and in 3 events it is above the line.

In Figure 4 we investigate the relation between the slope of the fit for each IP shock (as in Fig. 3) and (1) the density compression ratio, H, and (2) $V = V_s \sec(\theta_{Bn})$, which is the shock speed in the upstream solar wind frame along the upstream magnetic field direction. We selected these shock parameters merely because the former provides information about the strength of the shock and the latter is often used as a proxy for the injection threshold speed (Tsurutani & Lin 1985; Tylka & Lee 2006). Although there is a hint of correlation in Figure 4*a* (a correlation coefficient $r = -0.427$ represents an ~8% chance of being exceeded by a pair of uncorrelated quantities), we remark that this sample is too small to be statistically significant. Likewise, even though the correlation in Figure 4*b* is poor ($r = 0.098$ represents a 71% chance of being exceeded by a pair of uncorrelated parameters), it is possible that our sample could contain two distinct groups of events with opposite dependence on V_s with a possible break point at ~750 km s^{-1}. We also tried to find a correlation between the slope and θ_{Bn} (not shown), but without success.

Figure 5 shows the relationship between the 0.25–0.8 ^{3}He/^{4}He and Fe/C ratios measured during IP shock events and those measured upstream of the shocks. From Figure 5 we note that both the ^{3}He/^{4}He ratio and the Fe/C ratio in 11 of the 18 IP shock events are depleted relative to the corresponding upstream values. In two events, the IP shock-associated ^{3}He/^{4}He ratio is slightly enhanced, while that observed during the remaining five events is similar to the corresponding upstream value. In contrast, the Fe/C ratio in six IP shock events is similar to that observed upstream of the shocks, and for one event it is slightly enhanced.

4. DISCUSSION

Our survey of the abundances of 0.25–0.8 MeV nucleon^{-1} He$^+$, ^{3}He, and heavy ions from C-Fe during 18 IP shock events shows the following:

1. The ^{3}He and He$^+$ ions are accelerated by all of the 18 IP shocks with relative abundances significantly enhanced by factors of ~3–74 and ~400–15,000, respectively, over the corresponding solar wind values (^{3}He/^{4}He $\sim 0.000408 \pm 0.000025$, Gloeckler & Geiss 1998a; He$^+$/He^{2+} < 0.00005, Gloeckler & Geiss 1998b).
2. In 15 of the 18 events, the C-Fe abundances are systematically depleted according to the ion's M/Q ratio when compared with those of the ambient suprathermal population measured upstream of the shocks. In 7 out of 12 events, the He$^+$ abundance also follows the same trend with M/Q as that exhibited by the C-Fe abundances.
3. There is no significant correlation between the M/Q-dependent depletion and the locally measured IP shock parameters, such as the density compression ratio, the shock speed in the upstream plasma frame, and θ_{Bn}.
4. In 11 events the ^{3}He/^{4}He and Fe/C ratios are depleted with respect to the ambient population.

4.1. *M/Q-dependent Acceleration of Suprathermal Ions from Multiple Sources*

Since the ^{3}He and He$^+$ ions are extremely rare in the solar wind, they serve as unique tracers of their source material; the ^{3}He ions come from prior flare activity (see Mason et al. 1999), while the He$^+$ ions are interstellar pickup ions (Möbius et al. 1985; Gloeckler et al. 1994). Consequently, their very presence in the accelerated population with relative abundances that are substantially enhanced over the corresponding solar wind values essentially confirms the suprathermal origin of the source population for all 18 of the CME-driven IP shocks studied here (e.g., Desai et al. 2001;

TABLE 1

INTERPLANETARY SHOCK EVENTS FOR THIS SURVEY

		SHOCK INTERVAL				UPSTREAM INTERVAL				SHOCK PARAMETERS[a]		
EVENT (1)	SHOCK ARRIVAL (UT) (2)	Sampling Time (UT) (3)	$^3He/^4He \times 10^{-2}$ (4)	$He^+/He^{2+} \times 10^{-2}$ (5)	Fe/O (6)	Sampling Time (UT) (7)	$^3He/^4He \times 10^{-2}$ (8)	$He^+/He^{2+} \times 10^{-2}$ (9)	Fe/O (10)	H (11)	V_s (km s^{-1}) (12)	θ_{Bn} (deg) (13)
						1997						
1[b].....	Nov 22, 0913	Nov 22, 0501–Nov 22, 1727	0.91 ± 0.17	5.88 ± 0.19	0.098 ± 0.025	Nov 15, 2255–Nov 18, 2255	0.65 ± 0.12	21.3 ± 1.1	0.41 ± 0.11	2.45 ± 0.16	158.8 ± 1.2	81.7 ± 3.3
						1998						
2.....	Aug 6, 0644	Aug 4, 1646–Aug 7, 0020	0.392 ± 0.045	23.26 ± 0.42	0.0531 ± 0.0069	Jul 30, 1153–Aug 2, 1153	2.25 ± 0.21	...	0.291 ± 0.067	2.29 ± 0.21	84.3 ± 2.5	84.7 ± 1.2
3.....	Sep 24, 2313	Sep 23, 1548–Sep 25, 2231	0.338 ± 0.026	2.883 ± 0.042	0.1683 ± 0.0055	Sep 20, 0256–Sep 22, 0256	1.87 ± 0.18	...	0.092 ± 0.036	2.13 ± 0.33	343.2 ± 8.9	74.3 ± 6.4
4.....	Oct 18, 1901	Oct 18, 0345–Oct 19, 0428	0.396 ± 0.064	4.81 ± 0.15	0.133 ± 0.012	Oct 13, 0000–Oct 16, 0000	14.1 ± 0.6	10.4 ± 0.6	0.97 ± 0.22	2.53 ± 0.25	82.4 ± 1.1	45.4 ± 1.5
						1999						
5[b].....	Jun 26, 1931	Jun 25, 0638–Jun 27, 0105	0.439 ± 0.028	8.534 ± 0.051	0.1059 ± 0.0026	Jun 19, 2231–Jun 22, 2231	9.16 ± 0.22	25.8 ± 1.7	0.926 ± 0.060	2.16 ± 0.13	145.3 ± 1.7	59.7 ± 3.4
6[b].....	Jul 6, 1425	Jul 5, 0151–Jul 7, 0136	2.18 ± 0.10	7.09 ± 0.14	0.434 ± 0.022	Jun 29, 1730–Jul 2, 1730	1.85 ± 0.07	14.9 ± 0.3	1.421 ± 0.060	1.94 ± 0.20	138 ± 4.1	50.7 ± 5.6
7.....	Aug 4, 0116	Aug 2, 2319–Aug 4, 0653	1.59 ± 0.13	10.55 ± 0.48	0.128 ± 0.017	Jul 28, 0607–Jul 30, 1807	2.07 ± 0.10	6.6 ± 0.2	0.165 ± 0.016	3.44 ± 0.32	75.0 ± 2.3	52.2 ± 1.2
8[b].....	Sep 22, 1209	Sep 22, 0610–Sep 22, 2059	0.345 ± 0.085	3.678 ± 0.069	0.0667 ± 0.0069	Sep 16, 0738–Sep 18, 1938	7.19 ± 0.18	...	0.274 ± 0.026	2.64 ± 0.68	149.2 ± 3.4	69.4 ± 3.6
						2000						
9[b].....	Apr 6, 1632	Apr 6, 0501–Apr 6, 2246	0.141 ± 0.032	12.004 ± 0.057	0.2063 ± 0.0074	Apr 1, 0046–Apr 4, 0046	15.4 ± 0.6	87.7 ± 3.3	1.72 ± 0.14	3.84 ± 1.25	278.1 ± 8.3	68.2 ± 5.1
10.....	Jun 23, 1227	Jun 22, 1623–Jun 24, 0026	0.280 ± 0.035	9.24 ± 0.17	0.0786 ± 0.0026	Jun 18, 0911–Jun 20, 0911	0.446 ± 0.028	3.1 ± 0.1	0.1045 ± 0.0047	2.56 ± 0.54	189.6 ± 7.9	52.6 ± 6.7
11.....	Jul 13, 0919	Jul 12, 1603–Jul 13, 2127	0.297 ± 0.041	6.431 ± 0.047	0.0894 ± 0.0032	Jul 9, 1327–Jul 11, 1327	1.08 ± 0.06	...	0.0954 ± 0.0070	2.01 ± 0.25	76 ± 11[c]	86.3 ± 13.4
12.....	Jul 19, 1449	Jul 19, 0454–Jul 20, 0302	0.370 ± 0.040	34.1 ± 2.7	0.1033 ± 0.0038	Jul 14, 1845–Jul 16, 1845	0.163 ± 0.017	2.4 ± 0.05	0.586 ± 0.010	3.23 ± 0.65	153.6 ± 5.6	60.4 ± 4.2
13.....	Jul 28, 0910	Jul 28, 0726–Jul 28, 1921	0.96 ± 0.19	32.3 ± 3.7	0.246 ± 0.040	Jul 22, 1305–Jul 24, 1305	0.758 ± 0.034	...	0.1623 ± 0.0056	1.80 ± 0.12	122.0 ± 3.1	50.3 ± 3.1
14.....	Aug 11, 1811	Aug 10, 1724–Aug 12, 0554	0.437 ± 0.044	75.49 ± 0.89	0.1336 ± 0.0057	Aug 6, 0321–Aug 8, 0321	5.43 ± 0.21	13.2 ± 0.5	0.211 ± 0.020	2.24 ± 0.92	33.1 ± 9.7	89.7 ± 2.2
15.....	Sep 6, 1613	Sep 5, 0242–Sep 7, 0927	0.118 ± 0.015	2.138 ± 0.029	0.0767 ± 0.0020	Aug 31, 0310–Sep 3, 0310	3.46 ± 0.17	4.2 ± 0.3	0.337 ± 0.044	3.02 ± 0.34	154.3 ± 1.8	69.4 ± 3.1
16.....	Sep 17, 1657	Sep 16, 2037–Sep 18, 0705	0.956 ± 0.054	24.781 ± 0.083	0.4343 ± 0.0083	Sep 12, 1406–Sep 14, 0206	0.340 ± 0.025	29.9 ± 0.2	0.4612 ± 0.0060	1.37 ± 0.11	...	77.6 ± 2.5
17.....	Oct 5, 0240	Oct 4, 2233–Oct 5, 1023	3.02 ± 0.49	7.08 ± 0.44	0.471 ± 0.058	Sep 29, 1853–Oct 1, 1853	16.3 ± 1.0	8.3 ± 0.8	1.60 ± 0.19	2.29 ± 0.19	181.7 ± 1.9	72.7 ± 2.2
18[b].....	Oct 12, 2234	Oct 12, 0138–Oct 13, 2200	2.63 ± 0.14	17.57 ± 0.18	0.2049 ± 0.0089	Oct 6, 0140–Oct 9, 0140	6.52 ± 0.95	...	2.67 ± 0.60	2.43 ± 0.24	202.5 ± 6.6	71.6 ± 2.6

NOTES.—Col. (1): Number. Col. (2): Shock arrival time at *ACE* or *WIND* (accurate to the nearest minute). Col. (3): Shock interval sampling time. Cols. (4)–(6): $^3He/^4He$, He^+/He^{2+}, and Fe/O in the 0.25–0.80 MeV nucleon^{-1} energy range during the shock interval. Col. (7): Upstream interval sampling time. Cols. (8)–(10): $^3He/^4He$, He^+/He^{2+}, and Fe/O in the 0.25–0.80 MeV nucleon^{-1} energy range during the upstream interval. Col. (11): Density compression ratio. Col. (12): Shock speed in upstream plasma frame. Col. (13): Shock normal angle (given as $180^\circ - \theta_{Bn}$ if $\theta_{Bn} > 90^\circ$).

[a] From the MIT Space Plasma Group.

[b] Shock parameters measured at *WIND*.

[c] Shock speed not well determined.

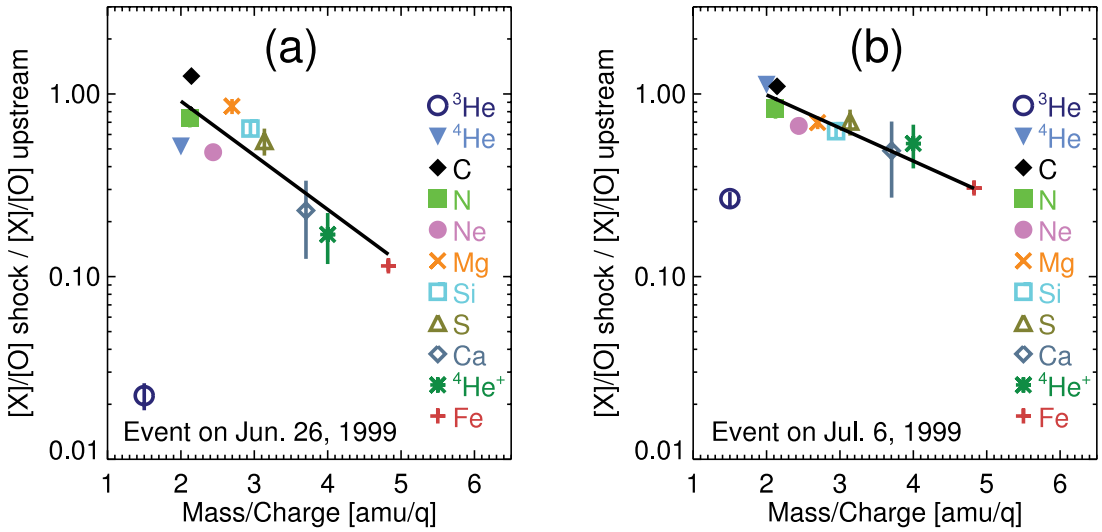

FIG. 3.—Shock to upstream abundance ratios normalized to oxygen as a function of the average M/Q ratio in gradual SEPs for (*a*) event 5 and (*b*) event 6 of Table 1. The line is a fit that does not include ^{3}He.

Kucharek et al. 2003). Note also that He^+ pickup ions have a very different phase space distribution than other suprathermal heavy ions.

Desai et al. (2003) showed that the C-Fe abundances averaged over 72 IP shock events had a negative dependence on the M/Q ratio when compared with the values averaged over upstream intervals of the same 72 IP shocks. Thus, our study extends the earlier work of Desai et al. and Kucharek et al. in two important ways: (1) the same IP shock can routinely accelerate ions from different sources, and (2) on a case-by-case basis, the abundances of C-Fe and He^+ are systematically depleted according to the ion's M/Q ratio when compared with the corresponding abundances measured in the ambient suprathermal ion population upstream of the shocks. Furthermore, even though the heavy ions C-Fe and pickup He^+ clearly originate from different sources, their relative abundances in the accelerated populations are nonetheless organized by the same simple rigidity- or M/Q-dependent fractionation processes in which ions with higher rigidity or M/Q ratio are accelerated less efficiently than those with lower M/Q ratio, at least when compared with a preexisting particle distribution in the same energy range.

Since such M/Q-dependent fractionation processes are consistent with predictions of diffusive shock acceleration models (see, e.g., Zank et al. 2005; Lee 2005), the heavy ion composition might be expected to exhibit larger fractionation effects at stronger shocks. However, we found that the systematic M/Q-dependent fractionation in IP shock abundances did not exhibit any clear dependence on the locally measured shock parameters. One possible reason is that the shock parameters are determined locally, while the IP shocks probably accelerated ions from the Sun en route to 1 AU. Thus, our IP shock–associated time intervals could also contain particles that may have been accelerated by the same IP shock at earlier times when it was probably stronger and had different orientation. Indeed, such poor correlations between the accelerated ion populations and the local shock parameters have been observed for decades (e.g., van Nes et al. 1984; Tsurutani & Lin 1985; Desai et al. 2004; Ho et al. 2005) and are not likely to be fully understood without using

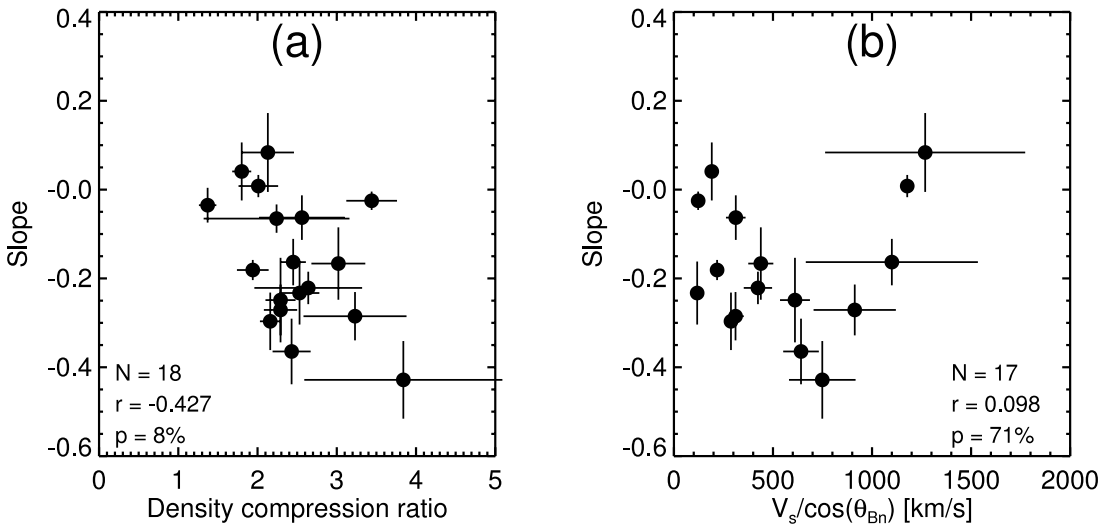

FIG. 4.—Slope of the fit (in Fig. 3) for all the events as a function of (*a*) the density compression ratio and (*b*) the injection speed. See Table 1 for the shock parameters. N is the number of events, r is the correlation coefficient, and p is the probability that a random distribution exceeds the correlation.

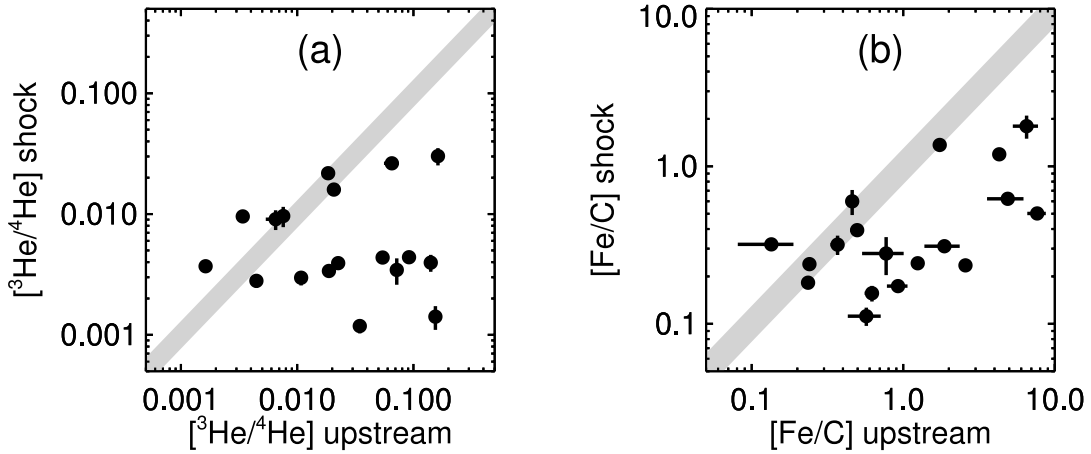

FIG. 5.—The 0.25–0.8 MeV nucleon^{-1} (*a*) ^{3}He/^{4}He and (*b*) Fe/C ratios at 18 IP shocks vs. those measured upstream. The gray band identifies events that exhibit a one-to-one relationship within ±30%. The data points mostly lie below the band [11 for (*a*) and (*b*)] or within the band [5 for (*a*) and 6 for (*b*)], and very few lie above it [2 for (*a*) and 1 for (*b*)]. (*a*) and (*b*) both suggest a depletion of the shock-accelerated population with respect to the upstream population.

multidimensional time-dependent modeling of individual IP shock events starting from the CME launch time at the Sun.

4.2. *Acceleration of* ^{3}He

Our results also show that the ^{3}He abundances when normalized to the upstream values do not follow the same systematic M/Q-dependent trend as that exhibited by the C-Fe and He^+ abundances. Furthermore, we find that the ^{3}He/^{4}He ratio measured at IP shocks is significantly depleted when compared with that measured upstream of the shocks. In many cases, the depletion factors for the ^{3}He abundance are larger than those seen for the higher rigidity Fe. This is puzzling, since the above-mentioned rigidity-dependent shock acceleration processes should have enhanced the ^{3}He abundance relative to the source population.

There are at least three possible explanations that could account for this result. First, the ^{3}He is somehow accelerated less efficiently than predictions of simple rigidity-dependent diffusive shock acceleration mechanisms. For instance, we note that the gyroradius of ^{3}He lies between that of the proton and the ^{4}He. Since both the protons and the ^{4}He are significantly more abundant than the ^{3}He, the former two species could damp some or most of the waves that resonate with the ^{3}He. This hypothetical situation would be clearly opposite to that which is believed to occur during the impulsive SEP events, where the postulated existence of waves that resonate only with the ^{3}He ions accelerate them more efficiently and result in large enhancements (e.g., Fisk 1978; Temerin & Roth 1992; Paesold et al. 2003). Despite the fact that measurements of power spectra at IP shocks are sparse, the experimental evidence published so far (e.g., Kennel et al. 1986; Bamert et al. 2004) does not seem to support this explanation. Also, model calculations of accelerated energetic ions and IP Alfvén waves (e.g., Ng et al. 2003) do not seem to show a damping effect. This explanation is therefore ruled out.

A second explanation could be related to the fact that particles from impulsive flare events are often injected along fairly narrow ranges in heliolongitude (Mazur et al. 2000). This would add another possibility for variation that is not present in the He^+, which is spatially comparatively uniform (e.g., Gloeckler & Geiss 1998b). In this case, the ^{3}He abundance could vary over timescales comparable to or shorter than the time interval that separates the shock and the upstream intervals. However, along with the ^{3}He, impulsive SEP events are also likely to contribute heavy ions from C-Fe to the seed population (see Desai et al. 2003, 2004). Since we used the same upstream intervals for inferring the abundances of the proxy seed population, this scenario would then require that only the ^{3}He behave oddly while all the rest of the heavy ions get systematically ordered by their M/Q ratio. On the basis of these arguments we think that this explanation is also unlikely, at least in the cases where a strong M/Q-dependent effect is observed.

A third, perhaps more simple, explanation is that even though the ~0.5 MeV nucleon^{-1} C-Fe and the He^+ abundances measured during the upstream intervals do appear to provide a reasonable proxy for those measured in the seed population, the corresponding upstream ^{3}He abundance does not represent that of the source population. This could be related to the results of Mason et al. (2002), which showed that the spectral shapes of ^{3}He and ^{4}He in the same impulsive SEP event are often significantly different from each other, such that the ^{3}He/^{4}He ratios could differ by factors of ~10 over a relatively small energy range. Of particular interest are the events where (1) the ^{3}He and

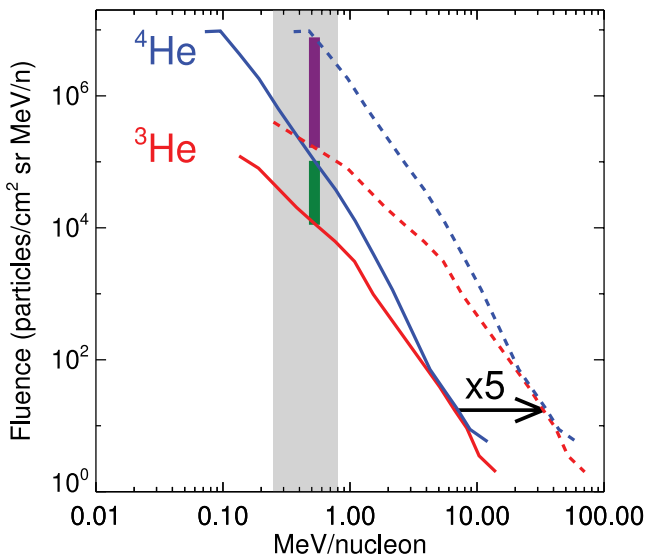

FIG. 6.—The ^{3}He and ^{4}He fluences (*solid lines*) for the 2000 September 27 event plotted vs. energy per nucleon (adapted from Mason et al. 2002). We shift the curves arbitrarily by a factor of 5 in energy, reflecting the effects of shock acceleration. The green and purple lines represent the ^{4}He/^{3}He ratios at ~0.5 MeV nucleon^{-1} for the "seed" and "accelerated" populations, respectively. Due to the different spectral shapes, the ^{3}He in the accelerated population is depleted with respect to the seed population.

^{4}He spectra behave as power laws, but the ^{3}He spectra are significantly harder than the ^{4}He spectra, as shown in Figure 6 (adapted from Mason et al. 2002); and (2) the ^{3}He spectra are curved and turn over around $\sim$0.4 MeV nucleon^{-1}, while the ^{4}He spectra continue as power laws down to the lowest energies.

In order to illustrate the potential effects of reaccelerating such unusual seed spectra, we shifted them arbitrarily by a factor of 5 in energy, reflecting the possible effects of shock acceleration (e.g., Kocharov & Torsti 2003; Desai et al. 2004; Li & Zank 2005). The vertical line can be used to infer the $\sim$0.5 MeV nucleon^{-1} ^{3}He/^{4}He in the seed population and the shock-accelerated population. This simple analysis clearly shows that if the IP shocks encountered and reprocessed such ^{3}He and ^{4}He distributions en route to Earth, then the $\sim$0.5 MeV nucleon^{-1} ^{3}He/^{4}He ratio measured upstream of the shocks could be substantially different from that at even slightly lower energies in the source population.

We remark that this explanation is also valid if the ^{3}He spectrum in the seed population is curved, provided that it turns over around or above our lower energy range, i.e., $\sim$0.35 MeV nucleon^{-1}. Note that Mason et al. (2002) did indeed report that in the case of events with curved ^{3}He spectra, they tended to turn over around $\sim$0.4 MeV nucleon^{-1}. Currently, however, owing to insufficient counting statistics and/or poor mass resolution of ULEIS, we are unable to directly measure the distribution functions of ^{3}He in the seed population below $\sim$0.35 MeV nucleon^{-1}. This implies that our suggested explanation cannot be fully tested without undertaking detailed case studies and combining them with sophisticated modeling of shock acceleration and transport using realistic distributions for the ^{3}He as inputs for the suprathermal seed population.

In any case, it would be very useful to model and simulate these events in order to see what we can learn about the injection and acceleration of the heavy ions. Moreover, a wave spectrum analysis could also provide useful information.

We would like to thank Berndt Klecker, Charles Smith, and Thomas Zurbuchen for very interesting discussions and ideas on this topic. The work at SwRI is partly supported by NASA SEC GI grant NNG05GM88G. We acknowledge the use of shock parameters from http://space.mit.edu/home/jck/shockdb/shockdb.html.

REFERENCES

Bamert, K., Kallenbach, R., Ness, N. F., Smith, C. W., Terasawa, T., Hilchenbach, M., Wimmer-Schweingruber, R. F., & Klecker, B. 2004, ApJ, 601, L99
Desai, M. I., Mason, G. M., Dwyer, J. R., Mazur, J. E., Gold, R. E., Krimigis, S. M., Skoug, R. M., & Smith, C. W. 2003, ApJ, 588, 1149
Desai, M. I., Mason, G. M., Dwyer, J. R., Mazur, J. E., Smith, C. W., & Skoug, R. M. 2001, ApJ, 553, L89
Desai, M. I., et al. 2004, ApJ, 611, 1156
Fisk, L. A. 1978, ApJ, 224, 1048
Forman, M. A., & Webb, G. M. 1985, in Collisionless Shocks in the Heliosphere: Reviews of Current Research, ed. B. T. Tsurutani & R. G. Stone (Geophys. Monogr. 34; Washington: AGU), 91
Gloeckler, G., & Geiss, J. 1998a, Space Sci. Rev., 84, 275
———. 1998b, Space Sci. Rev., 86, 127
Gloeckler, G., et al. 1994, J. Geophys. Res., 99, 17637
Ho, G. C., Roelof, E. C., & Mason, G. M. 2005, ApJ, 621, L141
Kennel, C. F., Corniti, F. V., Scarf, F. L., Livesey, W. A., Russell, C. T., & Smith, E. J. 1986, J. Geophys. Res., 91, 11917
Klecker, B., Scholer, M., Hovestadt, D., Gloeckler, G., & Ipavich, F. M. 1981, ApJ, 251, 393
Klecker, B., et al. 1999, in Proc. 26th Int. Cosmic Ray Conf. (Salt Lake City), 6, 83
———. 2000, in AIP Conf. Proc. 528, Acceleration and Transport of Energetic Particles Observed in the Heliopshere, ed. R. A. Mewaldt et al. (New York: AIP), 135
———. 2003, in Proc. 28th Int. Cosmic Ray Conf. (Tsukuba), 3277
Kocharov, L., & Torsti, J. 2003, ApJ, 586, 1430
Kucharek, H., et al. 2003, J. Geophys. Res., 108, LIS 15-1
Lario, D., Decker, R. B., Livi, S., Krimigis, S. M., Roelof, E. C., Russell, C. T., & Fry, C. D. 2005, J. Geophys. Res., 110, A09S11
Lee, M. A. 1983, J. Geophys. Res., 88, 6109
———. 2005, ApJS, 158, 38
Li, G., & Zank, G. P. 2005, Geophys. Res. Lett., 32, L02101
Mason, G. M., Mazur, J. E., & Dwyer, J. R. 1999, ApJ, 525, L133
Mason, G. M., et al. 1998, Space Sci. Rev., 86, 409
———. 2002, ApJ, 574, 1039
Mazur, J. E., Mason, G. M., Dwyer, J. R., Giacalone, J., Jokipii, J. R., & Stone, E. C. 2000, ApJ, 532, L79
Möbius, E., Hovestadt, D., Klecker, B., Scholer, M., Gloeckler, G., & Ipavich, F. M. 1985, Nature, 318, 426
Möbius, E., et al. 1998, Space Sci. Rev., 86, 449
———. 1999, Geophys. Res. Lett., 26, 145
———. 2000, in AIP Conf. Proc. 528, Acceleration and Transport of Energetic Particles Observed in the Heliopshere, ed. R. A. Mewaldt et al. (New York: AIP), 131
Ng, C. K., Reames, D. V., & Tylka, A. J. 2003, ApJ, 591, 461
Paesold, G., Kallenbach, R., & Benz, A. O. 2003, ApJ, 582, 495
Stone, E. C., Frandsen, A. M., Mewaldt, R. A., Christian, E. R., Margolies, D., Ormes, J. F., & Snow, F. 1998, Space Sci. Rev., 86, 1
Temerin, M., & Roth, I. 1992, ApJ, 391, L105
Tsurutani, B. T., & Lin, R. P. 1985, J. Geophys. Res. 90, 1
Tylka, A. J., & Lee, M. A. 2006, ApJ, 646, 1319
Tylka, A. J., Reames, D. V., & Ng, C. K. 1999, Geophys. Res. Lett., 26, 2141
van Nes, P., Reinhard, R., Sanderson, T. R., Wenzel, K.-P., & Zwickl, R. D. 1984, J. Geophys. Res., 89, 2122
Zank, G. P., Li, G., Florinski, V., Hu, Q., Lario, D., & Smith, C. W. 2005, J. Geophys. Res., 111, A6